Sem1 is a functional component of the nuclear pore complex–associated messenger RNA export machinery

Marius Boulos Faza,[1,2] Stefan Kemmler,[1] Sonia Jimeno,[3] Cristina González-Aguilera,[3] Andrés Aguilera,[3] Ed Hurt,[4] and Vikram Govind Panse[1]

[1]Institute of Biochemistry, ETH Zürich, CH-8093 Zürich, Switzerland
[2]Molecular Life Sciences Program, Life Sciences Zurich, CH-8057 Zurich, Switzerland
[3]Centro Andaluz de Biología Molecular y Medicina Regenerativa, 41092 Sevilla, Spain
[4]Biochemie-Zentrum Heidelberg, Universität Heidelberg, D-69120 Heidelberg, Germany

The evolutionarily conserved protein Sem1/Dss1 is a subunit of the regulatory particle (RP) of the proteasome, and, in mammalian cells, binds the tumor suppressor protein BRCA2. Here, we describe a new function for yeast Sem1. We show that *sem1* mutants are impaired in messenger RNA (mRNA) export and transcription elongation, and induce strong transcription-associated hyperrecombination phenotypes. Importantly, Sem1, independent of the RP, is functionally linked to the mRNA export pathway. Biochemical analyses revealed that, in addition to the RP, Sem1 coenriches with components of two other multisubunit complexes: the nuclear pore complex (NPC)-associated TREX-2 complex that is required for transcription-coupled mRNA export, and the COP9 signalosome, which is involved in deneddylation. Notably, targeting of Thp1, a TREX-2 component, to the NPC is perturbed in a *sem1* mutant. These findings reveal an unexpected nonproteasomal function of Sem1 in mRNA export and in prevention of transcription-associated genome instability. Thus, Sem1 is a versatile protein that might stabilize multiple protein complexes involved in diverse pathways.

Introduction

In eukaryotes, RNA polymerase II (RNAPII)-driven production of mRNAs in the nucleus initiates gene expression. The nascent pre-mRNAs are processed and matured into mRNAs by several protein complexes that are loaded onto transcription sites via their interaction with the C-terminal domain of RNAPII (for reviews see Reed and Cheng, 2005; Sommer and Nehrbass, 2005; Cole and Scarcelli, 2006). Processing and maturation events include the 5′ capping and splicing, and 3′ polyadenylation of the pre-mRNAs. Further, these steps are coupled to the dynamic interaction of mRNAs with several proteins, including export factors that facilitate their transport through the nuclear pore complex (NPC) into the cytoplasm. Studies over the past years have revealed that all steps during gene expression, starting from gene activation to the nuclear export of mRNAs, are tightly coupled (Suntharalingam and Wente, 2003; Reed and Cheng, 2005; Sommer and Nehrbass, 2005; Köhler and Hurt, 2007).

In budding yeast, the THO–transcription export (TREX) complex and the Sac3–Thp1–Sus1–Cdc31 (TREX-2; also called THSC) complex are involved in transcription-coupled mRNA export (Köhler and Hurt, 2007). The THO–TREX complex is thought to be recruited to the elongating RNAPII via the THO subunits (Hpr1, Tho2, Mft1, and Thp2), which function in transcription and biogenesis of mRNA protein complexes (messenger ribonucleoproteins [mRNPs]). The additional TREX factors Sub2 and Yra1 are involved in recruiting the Mex67-Mtr2 export receptor to the mRNP, thereby coupling mRNP biogenesis with their nuclear export (for reviews see Aguilera, 2005; Reed and Cheng, 2005; Köhler and Hurt, 2007). TREX-2

M.B. Faza and S. Kemmler contributed equally to this paper.

Correspondence to Vikram Govind Panse: vikram.panse@bc.biol.ethz.ch

Abbreviations used in this paper: 5-FOA, 5-fluoroorotic acid; AID, activation-induced cytidine deaminase; ChIP, chromatin immunoprecipitation; CSN, COP9 signalosome; DSB, double-strand break; GANP, germinal center–associated nuclear protein; mRNP, messenger ribonucleoprotein; NPC, nuclear pore complex; PCI, proteasome-COP9-initiation factor; RNAPII, RNA polymerase II; RP, regulatory particle; *se*, synthetic enhanced; *sl*, synthetic lethal; ssDNA, single-stranded DNA; TAP, tandem affinity purification; TAR, transcription-associated recombination; TEV, tobacco etch viral protease; TREX, transcription export.

The Rockefeller University Press $30.00
J. Cell Biol. Vol. 184 No. 6 833–846
www.jcb.org/cgi/doi/10.1083/jcb.200810059

potentially coordinates Spt7-Ada2-Gcn5 acetyltransferase (SAGA)-mediated transcription of a subset of genes at the nucleoplasmic face of the NPC (Rodríguez-Navarro et al., 2004). An integral component of TREX-2 is Sac3, a multidomain protein that serves as a binding platform for other members of the complex. The N-terminal and middle domain (N+M) of Sac3 binds Thp1 and Mex67-Mtr2, whereas the C-terminal domain mediates its NPC targeting (Fischer et al., 2002) and recruits the centrin Cdc31 as well as Sus1 (Fischer et al., 2004). Recent works from several groups have demonstrated a requirement of TREX-2 in the dynamic repositioning of a subset of gene loci from the nuclear interior to the nuclear periphery upon their activation (Brickner and Walter, 2004; Casolari et al., 2004; Cabal et al., 2006; Taddei et al., 2006; Kurshakova et al., 2007).

In addition to their direct function in mRNA export, THO–TREX and TREX-2 play an important role in preventing transcription-associated genomic instability. Impaired components of both complexes induce transcription elongation defects, in particular for long and GC-rich DNA sequences (for review see Aguilera, 2005) and repeat-containing genes (Voynov et al., 2006). THO and TREX-2 mutants show defects that lead to hyper-recombination phenotypes via the cotranscriptional formation of RNA/DNA hybrids (R loops) between the emerging RNA and the transcribed single-stranded DNA (ssDNA; Huertas and Aguilera, 2003). R loops are likely to become obstacles for subsequent elongating RNAPIIs, thus impairing transcription elongation or generating mRNA-RNAPII-DNA tertiary structures that can obstruct replication, leading to genome instability (Aguilera and Gómez-González, 2008).

Sem1 is a small acidic protein that is highly conserved among all eukaryotic species. *SEM1* was originally isolated as a multicopy suppressor of exocyst mutants in budding yeast (Jäntti et al., 1999). Mutations in Sem1 lead to several pleiotropic phenotypes such as defects in exocytosis, pseudohyphal growth, and defects in the cell cycle (Jäntti et al., 1999; Marston et al., 1999). Genetic screens and proteomic approaches identified Sem1 as a component of the lid subcomplex of the 19S regulatory particle (RP) of the 26S proteasome in both budding yeast and humans (Funakoshi et al., 2004; Krogan et al., 2004; Sone et al., 2004; Jossé et al., 2006). Loss of Sem1 impairs the functional integrity of the proteasomal RP (Funakoshi et al., 2004); *sem1Δ* mutants show impaired ubiquitin-dependent protein degradation and accumulate poly-ubiquitinated proteins (Sone et al., 2004). Further, RP mutants, when combined with *sem1Δ*, show an increased sensitivity to UV radiation and DNA-damaging agents such as hydroxyurea, which suggests a role of the RP in DNA repair (Funakoshi et al., 2004; Krogan et al., 2004). Dss1, the mammalian homologue of Sem1, was discovered to be a BRCA2-binding protein (Marston et al., 1999) that specifically interacts with the C-terminal portion of BRCA2 (Yang et al., 2002). Dss1 has since been shown to be essential for BRCA2 function both in mammalian cells (Li et al., 2006; Gudmundsdottir et al., 2007) and in the fungus *Ustilago maydis* (Kojic et al., 2003; Kojic et al., 2005). Depletion of Dss1 in mammalian cells induces phenotypes similar to those seen in BRCA2-deficient cells, which is attributable to a defect in homology-directed repair of double-strand breaks (DSBs) by gene conversion (Gudmundsdottir et al., 2007).

In this study, we describe a new function for the budding yeast Sem1. We provide multiple lines of evidence that Sem1, as part of TREX-2, functions in mRNA export. Moreover, we show that Sem1 is specifically enriched in distinct protein complexes, namely the RP, COP9 signalosome (CSN), and TREX-2 that function in diverse pathways. Notably, we find that targeting of Thp1 to TREX-2 is severely affected in a *sem1Δ* mutant. These data suggest that Sem1 might contribute to the functional integrity of its target complexes and thereby impact diverse pathways.

Results

Previous studies in fission yeast demonstrated a requirement for Sem1/Dss1 in the export of poly(A)$^+$ RNA (Thakurta et al., 2005; Mannen et al., 2008). Notably, genetic and visual screens in budding yeast have uncovered a role for the E3-ubiquitin ligases Tom1 and Rsp5 in the nuclear export of mRNAs (Duncan et al., 2000; Neumann et al., 2003). Nevertheless, it has remained unclear whether Sem1/Dss1 as part of the ubiquitin–proteasome pathway is required for proper mRNA export or whether Sem1/Dss1 has an additional function in the mRNA export pathway. Therefore, we sought to address this issue in budding yeast using a combination of cell biological, genetic, and biochemical approaches.

Sem1 but not the RP is required for nuclear poly(A)$^+$ RNA export

We initiated our analysis by asking whether a budding yeast strain deficient for Sem1 (*sem1Δ*) exhibits nuclear accumulation of poly(A)$^+$ RNA. We assessed this phenotype by FISH using Cy3-labeled oligo (dT) probes. Nearly all the *sem1Δ* cells, when grown at 30°C, showed a nuclear accumulation of poly(A)$^+$ RNA (Fig. 1 A). This phenotype was also observed at 25°C and 37°C (not depicted). Furthermore, the nuclear accumulation of poly(A)$^+$ RNA was found to be comparable to TREX-2 deletion mutants (i.e., *thp1Δ* and *sac3Δ*; Fischer et al., 2002) but less severe than in the *mex67-5* strain at 37°C (Fig. 1 A).

Because Sem1 was previously identified as a nonessential, bona fide subunit of the RP, we tested whether deletion of other nonessential components also induces defects in poly(A)$^+$ RNA export. However, strains deficient in *PRE9*, *RPN10*, *RPN4*, *UBP6*, and *RPN9* were not found to accumulate poly(A)$^+$ RNA inside the nucleus (Figs. 1 B and S1 A). Using temperature-sensitive (*ts*) mutants (*cim3-1* and *cim5-1*), we tested whether impairment of essential components of the RP induced nuclear accumulation of poly(A)$^+$ RNA. Neither *cim3-1* nor *cim5-1* were found to show this phenotype at the restrictive temperature (Fig. 1 B). Finally, the treatment of the drug-permeable yeast strain *erg6Δ* (Lee and Goldberg, 1998) with the proteasomal inhibitor MG132 did not induce a nuclear accumulation of poly(A)$^+$ RNA (Fig. S1 B). Thus, Sem1 is the unique component of the RP that is required for proper nuclear export of poly(A)$^+$ RNA.

Sem1 interacts genetically with mRNA export factors

Next, we asked whether Sem1 is genetically linked to factors involved in mRNA export. We found that *sem1Δ* is indeed synthetic lethal (*sl*) or synthetic enhanced (*se*) in combination with

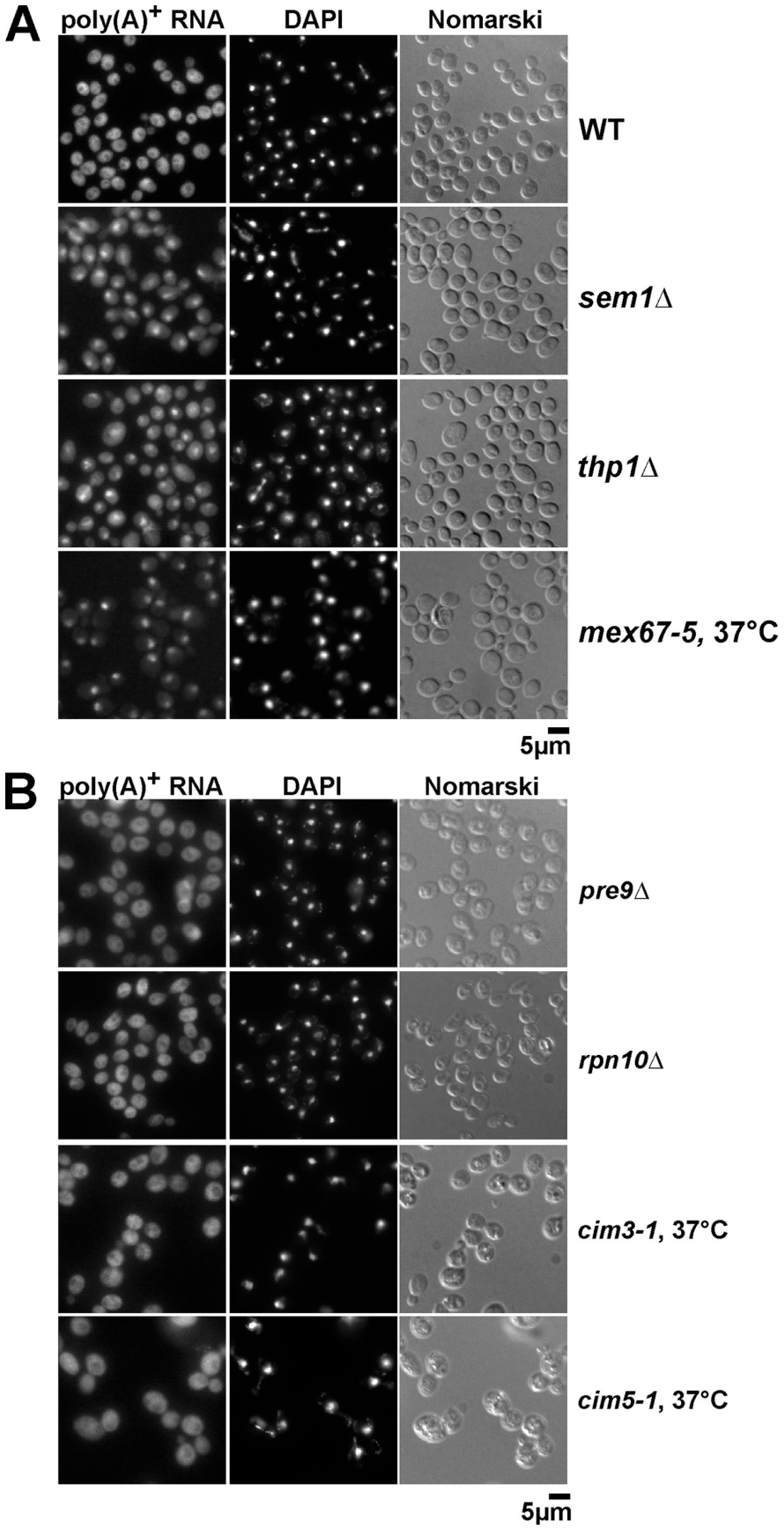

Figure 1. **Poly(A)+ RNA export is inhibited in *sem1Δ* but is not impaired in mutants of the RP.** (A) The depicted yeast strains were grown in YPD at 30°C; the localization of poly(A)+ RNA in the strains was assessed by in situ hybridization using Cy3-oligo $(dT)_{30}$, and DNA was stained with DAPI. The *mex67-5* strain was grown at 25°C and subsequently shifted to 37°C for 1 h. (B) The *cim3-1* and *cim5-1* were grown to logarithmic phase at 25°C and subsequently shifted to 37°C for 4 h. Other details were as in A.

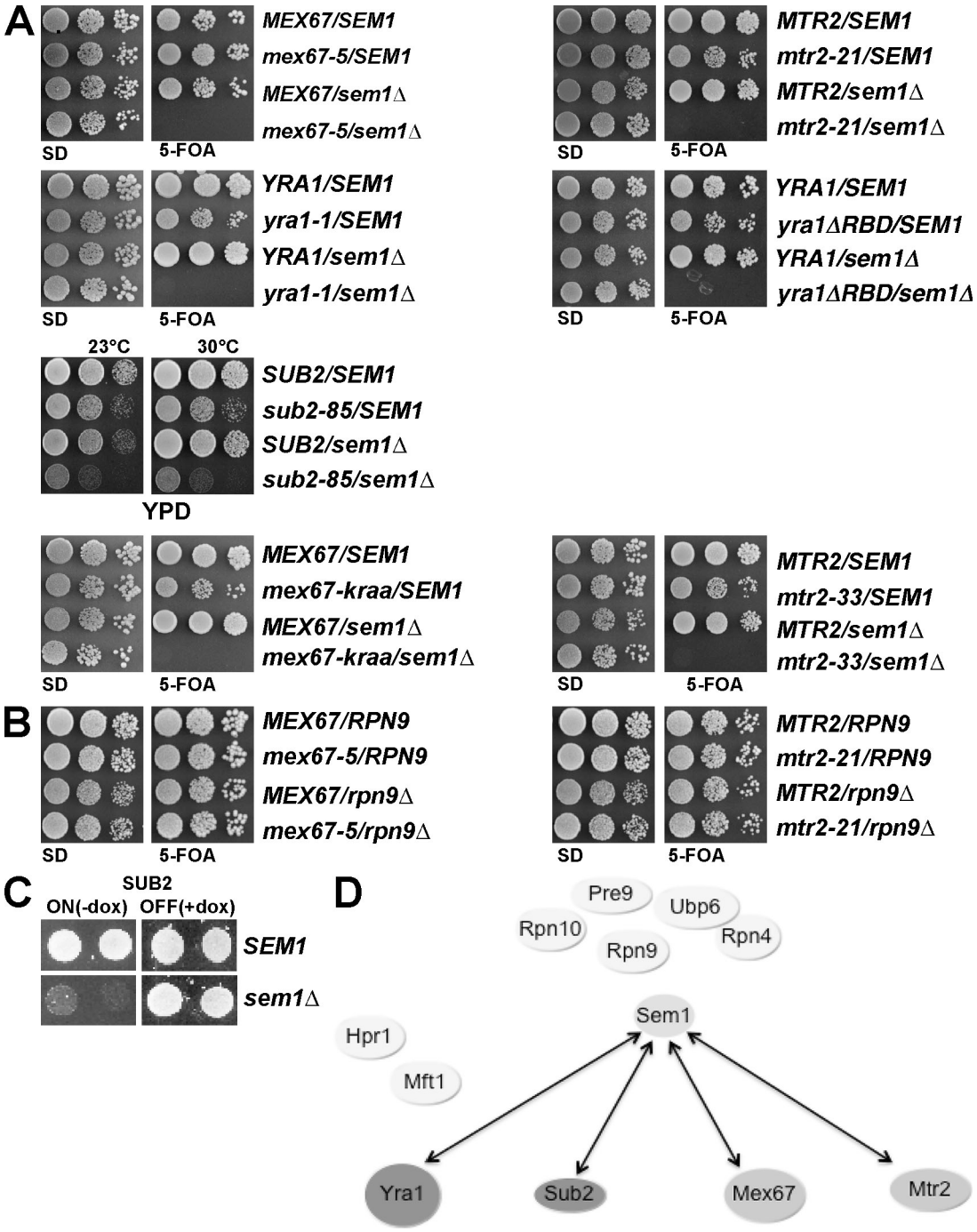

Figure 2. ***SEM1* is genetically linked to essential components of the mRNA export machinery.** (A and B) *sl* or *se* of the *sem1Δ* strain when combined with mutant alleles *mex67-5*, *mtr2-21*, *yra1ΔRBD*, *yra1-1*, and *sub2-85*. The *rpn9Δ* strain was used as a control. The strains carrying the indicated wild-type and mutant alleles were spotted in serial 10-fold dilutions onto 5-FOA plates (when *sl*) or YPD (when *se*) and incubated at 25°C and 30°C for 3–5 d. (C) The effect of *SUB2* overexpression on *sem1Δ*. Viability of wild-type (W303-1A) and *sem1Δ* isogenic strains transformed with the plasmid *Ptet-SUB2*, containing the *SUB2* gene under the control of a *tet* promoter, which is expressed in the absence of doxycyclin (dox). Transformants were spotted as 10-fold serial dilutions on selective medium with and without doxycyclin. Growth was analyzed after 4 d at 30°C. (D) Schematic representation of the genetic network between Sem1 and factors involved in transcription-coupled mRNA export. Arrows indicate *sl/se*; an absence of arrows indicates the lack of genetic links with Sem1.

impaired alleles of known mRNA export factors such as Mex67, Mtr2, Yra1, and Sub2 (Fig. 2 A). In contrast, other nonessential components of the RP (*rpn9Δ*, pre9Δ, *rpn4Δ*, *rpn10Δ*, and *ubp6Δ*), when combined with *mex67* and *mtr2* mutants, were not found to be *sl* or *se* (Figs. 2 B and S2, and not depicted). Notably, we found that overexpression of Sub2, a component of TREX, strongly inhibited growth of *sem1Δ*, but not of the RP mutants (Fig. 2 C and not depicted). Similar effects of increased Sub2 levels have been described previously in *sac3Δ*, *thp1Δ* and *sus1Δ* mutants (Gallardo, 2003; Gonzalez-Aguilera et al., 2008).

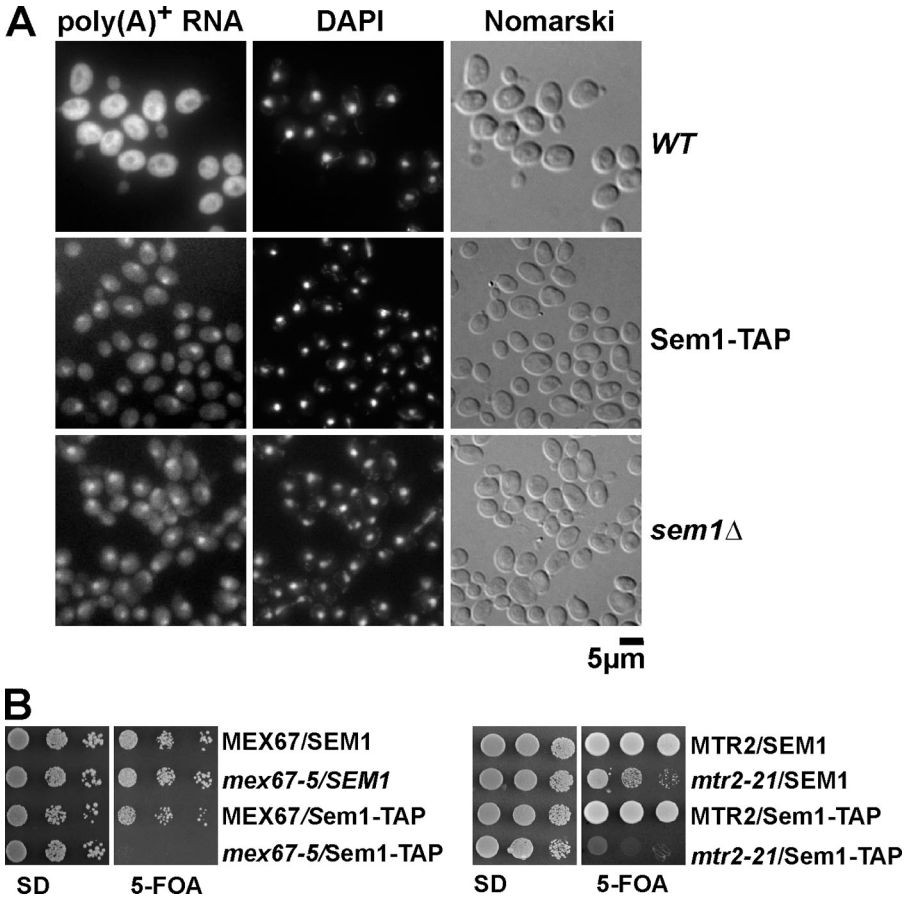

Figure 3. **Sem1-TAP is not functional in the mRNA export pathway.** (A) Wild-type and Sem1-TAP strains were grown in YPD at 30°C; the localization of poly(A)$^+$ RNA in the strains was assessed by in situ hybridization using Cy3-oligo (dT)^{30}, and DNA was stained with DAPI. (B) *sl* of the Sem1-TAP strain when combined with strains that contain mutant alleles *mex67-5* and *mtr2-21*. The strains carrying the indicated wild-type and mutant alleles were spotted in serial 10-fold dilutions onto synthetic dextrose complete medium + 5-FOA plates, and incubated at 30°C for 4 d.

However, THO mutants (*mft1Δ*, *hpr1Δ*), when combined with *sem1Δ*, do not exhibit synergistic growth defects (unpublished data). We conclude that Sem1, but not the RP, is functionally linked to specific components of the mRNA export pathway (summarized in Fig. 2 D).

Sem1 coenriches with the NPC-associated TREX-2

The sensitivity of *sem1Δ* to Sub2 overexpression points to a functional link between Sem1 and the TREX-2 complex, and raises the possibility of a direct physical association with TREX-2. Previously, Sem1–tandem affinity purification (TAP) was shown to only purify the RP; however, the functionality after the addition of a C-terminal TAP tag to Sem1 was not analyzed (Funakoshi et al., 2004; Krogan et al., 2004; Sone et al., 2004; Jossé et al., 2006). To address the possibility that the fusion protein is nonfunctional in the mRNA export pathway, we analyzed Sem1-TAP by FISH, using Cy3-labeled oligo (dT) and by genetic means. We found that like *sem1Δ*, the Sem1-TAP strain is defective in mRNA export (Fig. 3 A). Moreover, Sem1-TAP is *sl* when combined with *mex67* and *mtr2* alleles (Fig. 3 B) and sensitive to Sub2 overexpression (not depicted). Together, we conclude that Sem1-TAP is nonfunctional in the mRNA export pathway.

Hence, to investigate whether Sem1 associates with TREX-2, we directly purified this complex using Thp1-TAP and protein A–Sac3 as bait proteins. The tobacco etch viral protease (TEV) eluates were subjected to SDS-PAGE and Western analysis using antibodies directed against Sem1 and Rpt6, a core component of the RP. Rpn1-TAP and a yeast lysate containing no TAP-tagged bait protein served as positive and negative controls, respectively. These biochemical analyses show that Sem1 specifically coenriches with Thp1-TAP and protein A–Sac3 (Fig. 4, A and B). However, Sem1 is not found in any other protein complex involved in mRNA export such as THO–TREX (Mft1-TAP, Thp2-TAP) and the exosome (Rrp46-TAP; Fig. 4 A and not depicted). Importantly, Rpt6 was only detected in the Rpn1-TAP and not in any of the other purifications (Fig. 4 A). Thus, Sem1 coenriches with TREX-2 independently of the RP.

Previously, the N+M domain of Sac3 has been reported to interact with Thp1 and the mRNA export adaptor Mex67-Mtr2, whereas the NPC-targeting C domain of Sac3 interacts with Sus1 and Cdc31 (Fischer et al., 2002; Fischer et al., 2004). We performed purifications from yeast lysates containing protein A–Sac3, protein A–N+M–Sac3, and protein A-C–Sac3. We found that the N+M domain but not the C domain of Sac3 is required for coenrichment of Sem1 (Fig. 4 B). Next, we asked whether Sem1, like in the case of the RP, is a bona fide component of TREX-2. For this, protein A–Sac3 was purified from a strain containing Thp1-GFP and an untagged strain (negative control). A fraction of the TEV eluates were analyzed by SDS-PAGE, and Western analysis was performed using antibodies directed against GFP (to detect Thp1-GFP) and Sem1. The TEV

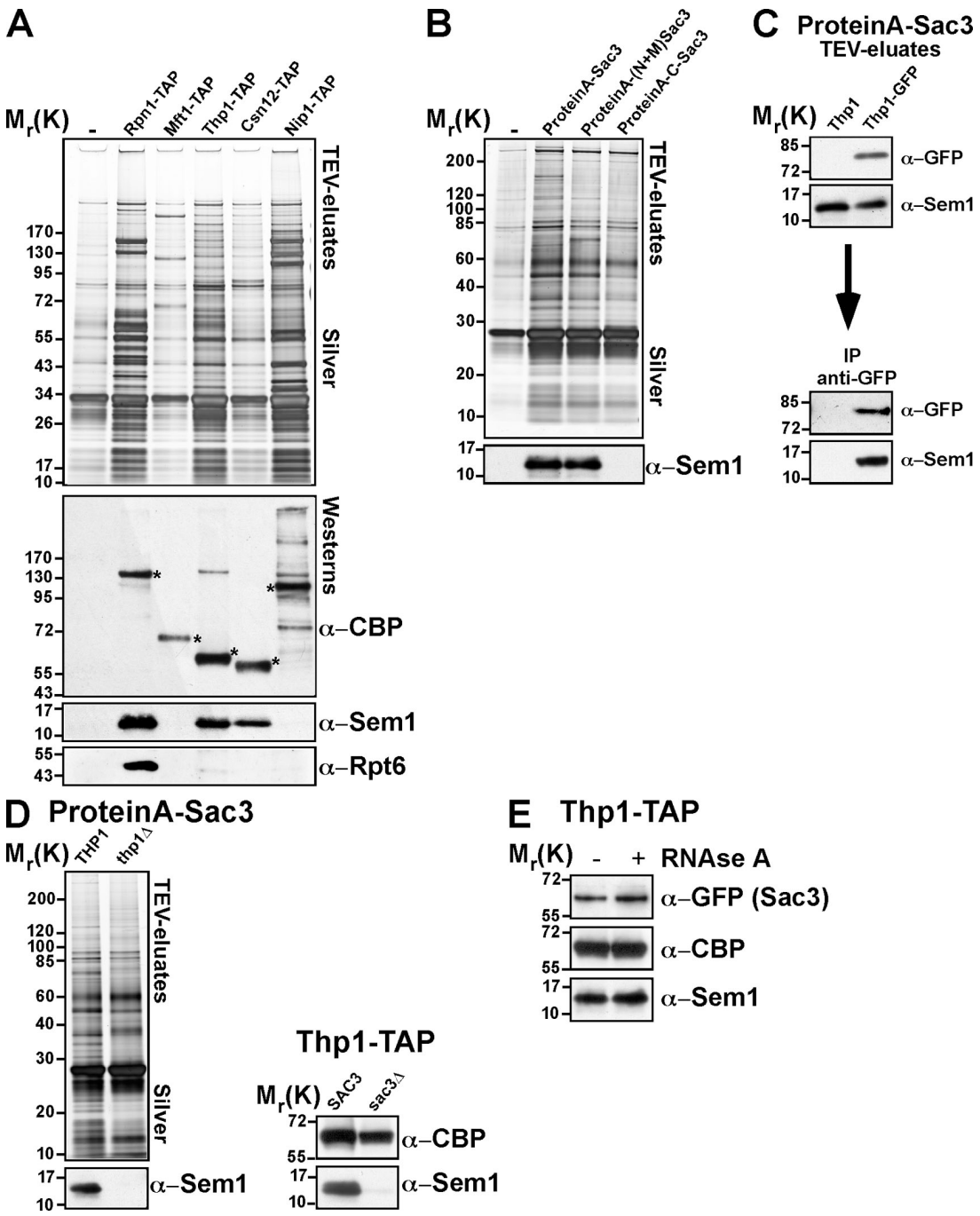

Figure 4. **Sem1 is a bona fide subunit of TREX-2.** (A and B) The indicated TAP- or protein A–tagged bait proteins were isolated from yeast lysates by affinity purification using an IgG-Sepharose. TEV eluates of purified bait proteins were separated on a 4–12% SDS–polyacrylamide gradient gel and subjected to silver staining. Western blot analysis of the purified protein complexes was performed with indicated antibodies against CBP, Sem1, and Rpt6. Asterisks indicate the positions of bait proteins. (C) In order to show that Sem1 is a stoichiometric component of TREX-2, sequential affinity purifications were performed. In the first step, protein A–Sac3 was purified from lysates derived from strains expressing Thp1-GFP and Thp1 (negative control) to isolate TREX-2. The bound material was released by TEV cleavage, and a part of the eluates was separated on a 4–12% SDS–polyacrylamide gradient gel, then analyzed by Western blotting using antibodies against GFP and Sem1 (top). In the second step, the rest of the TEV eluates were incubated with Sepharose coupled to anti-GFP antibodies. The bound material was eluted and separated on a 4–12% SDS–polyacrylamide gradient gel and analyzed by Western blotting using antibodies against GFP and Sem1 (IP anti-GFP, bottom). (D) Protein A–Sac3 and Thp1-TAP were isolated from yeast lysates from *thp1Δ* and *sac3Δ* strains by affinity purification using an IgG-Sepharose. Lysates derived from wild-type strains were used as controls. The bound material was released by TEV cleavage. TEV eluates of purified bait proteins were separated on a 4–12% SDS–polyacrylamide gradient gel and subjected to silver staining. Western blot analysis of the purified protein complexes was performed with indicated antibodies against CBP and Sem1. (E) Thp1-TAP was isolated from yeast lysates in which Sac3 was tagged with GFP by affinity purification using an IgG-Sepharose. The bound material was incubated with and without 20 µg/ml RNase A for 1 h. The IgG-Sepharose resin with the bound material was washed with 5 bed volumes of wash buffer. The bound TREX-2 was released by TEV cleavage, and the TEV eluates were separated on a 4–12% SDS–polyacrylamide gradient gel; Western analyses were performed using antibodies against GFP, CBP, and Sem1 to detect components of TREX-2.

eluates enriched both Thp1-GFP and Sem1 (Fig. 4 C, top). The rest of the TEV eluates were incubated with Sepharose beads that were coupled to anti-GFP antibodies. The bound material was eluted and subjected to SDS-PAGE and Western analysis. Sem1 was specifically enriched in the TEV eluates obtained from protein A–Sac3 purification that contained Thp1-GFP but not Thp1 (Fig. 4 C, bottom). Further, we analyzed the requirement for the enrichment of Sem1 with TREX-2. To this end, we purified Thp1-TAP from a *sac3Δ* strain and protein A–Sac3 from a *thp1Δ* strain. The presence of Sem1 in the TEV eluates was probed by Western analysis. Sem1 failed to coenrich in both purifications (Fig. 4 D). These biochemical data suggest that the enrichment of Sem1 with TREX-2 requires the presence of both Sac3 and Thp1. Importantly, the enrichment of Sem1 with TREX-2 was found to be insensitive to RNase A treatment (Fig. 4 E). Thus, Sem1 association with TREX-2 requires both Sac3 and Thp1, and is independent of its association with RNA. All together, these biochemical data strongly suggest that, like in the RP, Sem1 is a bona fide component of TREX-2.

Sem1 coenriches with Sac3–germinal center–associated nuclear protein (GANP) and PCI-associated module (PAM) domain–containing protein complexes

Previously, sequence analysis of individual subunits of the RP and TREX-2 had revealed one common feature: two subunits of each complex contain a Sac3-GANP domain and a PAM domain, respectively. The Sac3-GANP domains are present in Rpn12 (RP) and Sac3 (TREX-2), whereas Rpn3 (RP) and Thp1 (TREX-2) contain the PAM domains (Fig. 5; Ciccarelli et al., 2003; Scheel and Hofmann, 2005). Both domains are predicted to be α-helical and have been proposed to mediate protein–protein interactions (Ciccarelli et al., 2003). Notably, Csn12, a subunit of the CSN, has also been reported to contain a PAM domain (Fig. 5; Ciccarelli et al., 2003). Large-scale proteomic approaches had revealed a coenrichment of the Sac3-GANP domain containing protein Ypr045c in the Csn12-TAP purification (Krogan et al., 2006). Therefore, we asked whether Sem1 also coenriches with these components. Western analysis of Csn12-TAP (Fig. 4 A) and Ypr045c-TAP (not depicted) preparations show that this is indeed the case. Because the PAM domain is often found upstream of proteasome-COP9-initiation factor (PCI) domains, we investigated the ability of Sem1 to bind to PCI domains. We were unable to detect Sem1 in a Nip1 purification (Fig. 4 A), which coenriches eIF3, a PCI domain containing translation initiation factor. Therefore, we conclude that Sem1 specifically coenriches with at least three distinct protein complexes that contain Sac3-GANP and PAM domains.

Sem1 is required for proper targeting of Thp1 to the NPC in vivo

Previous studies have shown that the C-terminal domain of Sac3 is required for its anchorage to the NPC, whereas the N+M domain of Sac3 was shown to provide a docking platform for Thp1 (Fischer et al., 2002). We asked whether deletion of Sem1 affects the NPC localization of Sac3 and Thp1. For this, we

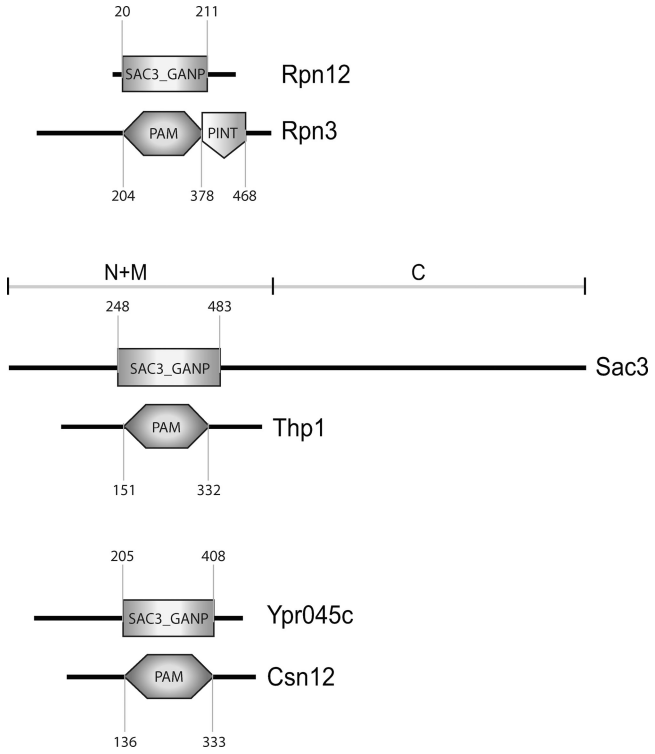

Figure 5. **Sac3-GANP and PAM domain protein pairs in budding yeast.** Sac3-GANP and PAM domain–containing proteins are part of three large multisubunit complexes: RP, TREX-2, and the CSN. The schematic of the proteins shows their domain organization. Sequence analysis was performed using the online program SMART (http://smart.embl-heidelberg.de/).

tagged both Sac3 and Thp1 at their C termini with GFP in *sem1Δ* strains at their genomic loci. As described previously, Thp1-GFP and Sac3-GFP have a punctate distribution at the nuclear periphery in wild-type cells (Fischer et al., 2002). In *sem1Δ* cells, the association of Thp1-GFP with the NPC is severely perturbed (Fig. 6 A). Furthermore, we observed an increase in cytoplasmic staining of Thp1-GFP in *sem1Δ* cells. However, the punctate staining of Sac3-GFP is only slightly affected in *sem1Δ* cells. Mislocalization of Thp1-GFP in *sem1Δ* cells is specific because we did not observe this phenotype in other deletion mutants of the RP (Fig. S3 A). Localization of the structural nucleoporin Nic96-GFP remained unaltered in a *sem1Δ* strain, which strongly suggests that NPCs remained intact (Fig. S3 B). Moreover, Western analysis of whole cell lysates showed no change in the levels of Thp1 in wild type and *sem1Δ* (Fig. 6 B). Finally, Thp1-TAP purification from a *sem1Δ* strain reproducibly revealed a reduced enrichment of Sac3-GFP as compared with the control strain that contained SEM1 (Fig. 6 C). Together, we conclude that Sem1 is required for efficient association of Thp1 with the NPC.

sem1Δ shows transcription-dependent hyper-recombination and transcriptional defects similar to *thp1Δ*, *sac3Δ*, and *sus1Δ* mutants

The data so far show that Sem1 interacts both functionally and physically with TREX-2. Hence, we wondered whether *sem1Δ* could induce similar transcription-associated recombination

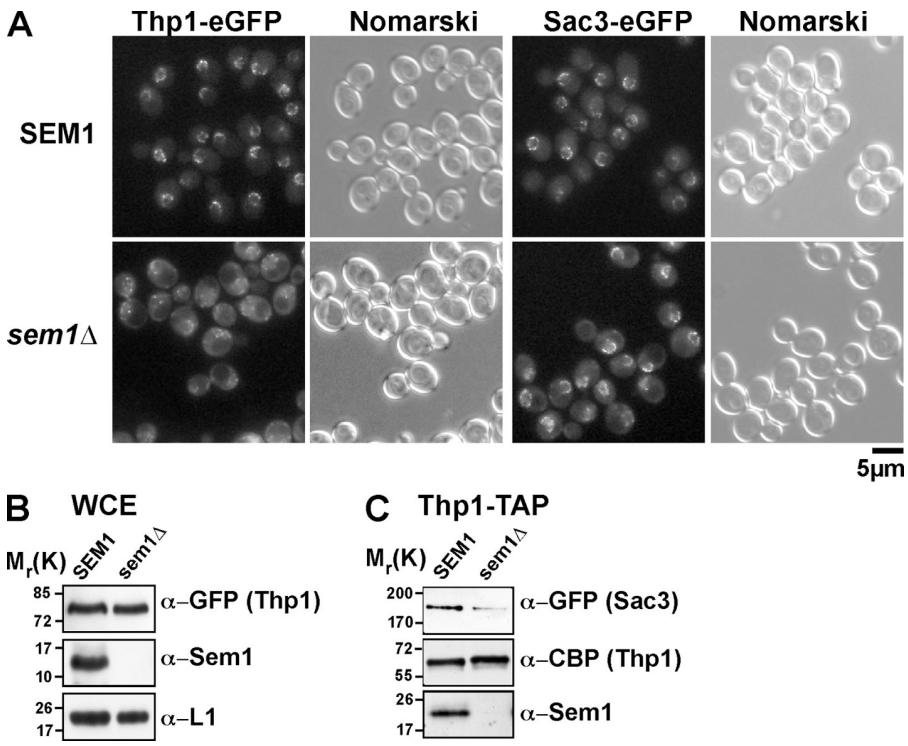

Figure 6. **Thp1 is inefficiently recruited to the NPC in *sem1Δ* cells.** (A) The depicted yeast strains were grown to logarithmic phase at 30°C. The localization of Thp1-GFP and Sac3-GFP in *sem1Δ* cells and the isogenic wild-type strain was visualized by fluorescence microscopy. (B) Whole cell extracts were prepared from Thp1-GFP in wild-type and sem1Δ strains. The extracts were analyzed by SDS-PAGE and subjected to Western analysis using anti-GFP antibodies. Ribosomal protein L1 was used as loading control. (C) Thp1-TAP purification was performed from SEM1 and *sem1Δ* strains in which Sac3 was tagged with GFP. TEV eluates were separated on a 4–12% SDS–polyacrylamide gradient gel, and Western blot analysis was performed with indicated antibodies against GFP (Sac3-GFP), CBP (Thp1-CBP), and Sem1.

(TAR) and transcription deficiency phenotypes that have been observed in *thp1Δ*, *sac3Δ*, and *sus1Δ* mutants (Aguilera and Gómez-González, 2008). Transcription through long and GC-rich genes like *LacZ* was found to be impaired in *thp1Δ* and *sac3Δ* mutants (Gallardo, 2003). To test whether this is also the case for *sem1Δ*, we analyzed gene expression in the pLAUR system that contains a 4.15-kb *lacZ-URA3* translational fusion under the control of the *tet* promoter (Jimeno et al., 2002). *sem1Δ* cells carrying the pLAUR system were unable to form colonies on synthetic medium lacking uracil (SC-Ura-Trp) and did not show β-galactosidase activity (Fig. 7 A), which indicates that they did not properly express the *lacZ-URA3* fusion. Northern analysis of *sem1Δ* showed decreased mRNA levels compared with the wild type (Fig. 7 A). This reduction was not caused by an impairment of transcription initiation at the *tet* promoter, as the expression of the pCM189-LEU2 system (short, GC-poor) was not affected in the *sem1Δ* mutant (Fig. 7 B). We asked whether Sem1-TAP, which still interacts with the RP but is defective in mRNA export, is able to properly express the *lacZ-URA3* fusion. As expected, Sem1-TAP was found to be defective in expressing the *lacZ-URA3* fusion (Fig. 7 C). Importantly, mutants of the RP (*rpn10Δ* and *pre9Δ*) carrying the pLAUR system were still able to support growth on synthetic medium lacking uracil (SC-Ura-Trp) and showed β-galactosidase activity (Fig. 7 A). Thus, Sem1, not as part of the RP, is required for proper expression of long GC-rich genes. Importantly, this phenotype was found to be very similar to that observed in *thp1Δ* and *sac3Δ* mutants.

For the analysis of TAR, we transformed the LNA and LNAT systems (see Fig. S4 for a scheme of the various recombination systems used), based on 0.6-kb *leu2* repeats into the *sac3Δ*, *thp1Δ sem1Δ*, Sem1-TAP, *pre9Δ*, and *rpn10Δ* mutant strains. The frequencies of recombination observed in the above mentioned strains were obtained by quantifying the number of revertants that grew on media lacking leucine. *sem1Δ* and Sem1-TAP strains exhibit a vast increase in recombination above wild-type levels (Fig. 8 A). To see whether this increase in recombination is dependent on transcription, we used the LNAT system, identical to LNA but with a transcriptional terminator located downstream of the *leu2Δ3′* fragment so that the intervening region is not transcribed. In this construct, recombination levels are found to resemble those seen in the wild type (Fig. 8 A), which suggests that the hyper-recombination phenotype of *sem1Δ* and Sem1-TAP is transcription dependent. To check further whether the phenotypes observed in *sem1Δ* mutants were independent of its RP function, we addressed whether mutants of the RP (*pre9Δ* and *rpn10Δ*) show similar recombination or transcription phenotypes. For the analysis of TAR, we used systems similar to those described above, based on 0.6-kb *leu2* repeats: LYΔNS in which transcription has to proceed through a long and GC-rich intervening sequence between the *leu2* repeats, and L that is identical to LYΔNS but without an intervening sequence between the repeats. Mutants of the RP did not show an increase in recombination in either system, whereas an increase in recombination was specifically observed in the LYΔNS system for Sem1-TAP and in mutants of TREX-2 (*thp1Δ* and *sac3Δ*; Fig. 8 B). These results are consistent with the fact that the Sem1-TAP strain is not able to properly transcribe the *LacZ-URA3* fusion of pLAUR and only reaches 37% of mRNA levels observed in the wild-type strain (Fig. 7 C), whereas the mutants of the RP did not show gene expression defects in the pLAUR system (Fig. 7 A). Altogether, these data strongly suggest that the observed hyper-recombination phenotypes in *sem1Δ* and Sem1-TAP are due to its association with TREX-2 and not linked to the role of Sem1 as part of the RP.

To further demonstrate this, we determined the effect of *sem1Δ* on recombination events in the L-*lacZ* and GL-*lacZ*

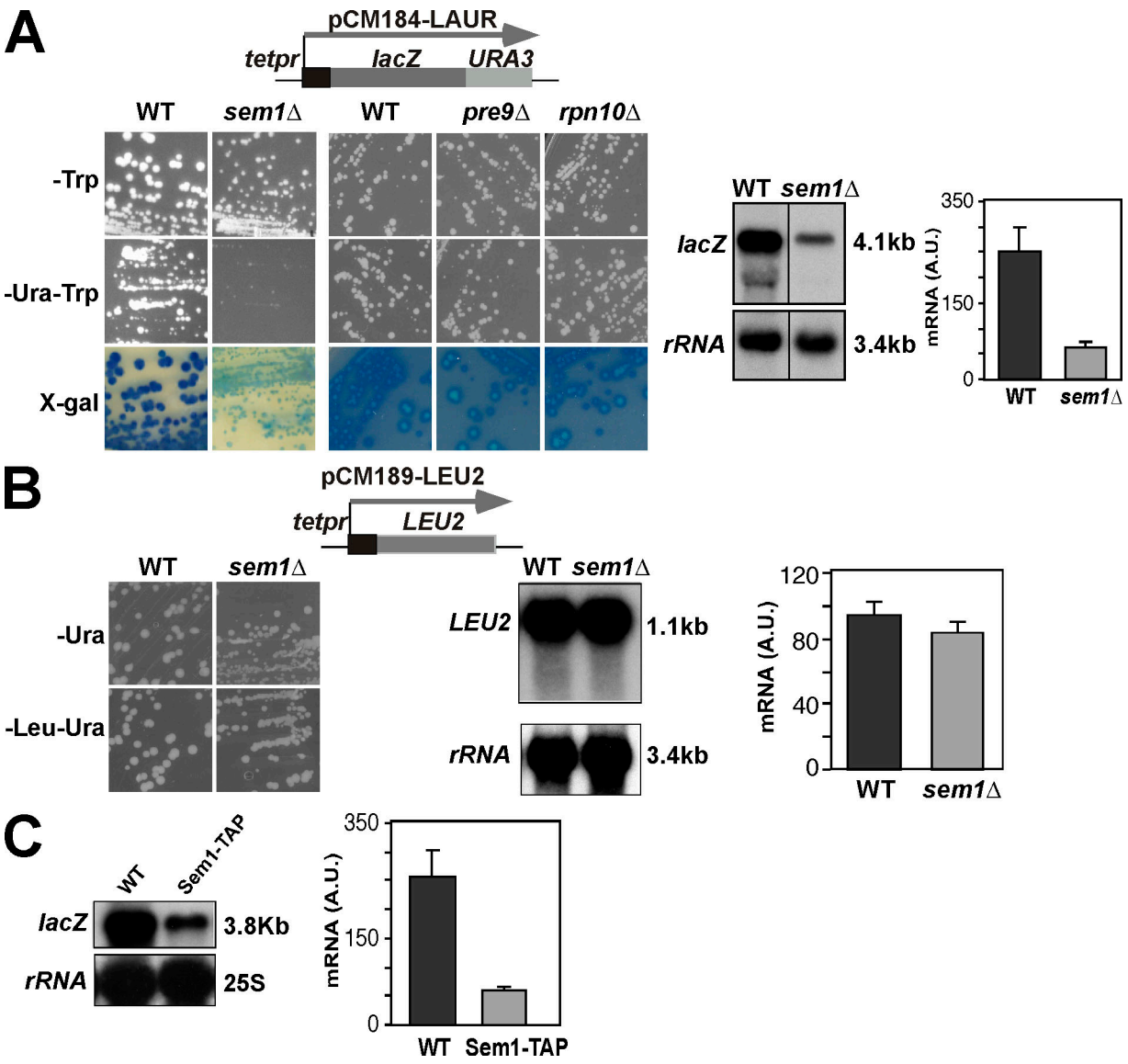

Figure 7. ***sem1Δ* and Sem1-TAP, but not mutants of the RP, are impaired in transcription of long, GC-rich genes.** Gene expression analysis of the pCM184-LAUR and pCM189-LEU2 constructs, as shown by analysis of the capacity of *sem1Δ* and the isogenic wild-type (W303-1A) strains carrying the *tetpr::lacZ-URA3* fusion to accumulate β-galactosidase and to form colonies on SD-Trp-Ura after 3 d at 30°C, as well as by Northern analysis. RNA was isolated from mid-log phase cultures. As a P^{32}-labeled DNA probe, we used the 3-kb BamHI–*lacZ* fragment and an internal 589-bp 25S rDNA fragment obtained by PCR. RNA levels in arbitrary units (A.U.) were normalized with respect to rRNA levels of each sample.

systems, based on the same 0.6-kb *leu2* direct repeats as before but flanking the *lacZ* open reading frame, in which the *leu2Δ3′* repeat was under the control of either its endogenous promoter or the inducible *GAL1* promoter. Studies were performed under conditions of low (*GAL1* promoter in 2% glucose), medium (*LEU2* promoter), and high levels of transcription (*GAL1* promoter in 2% galactose). The increase in recombination under low transcription conditions was less pronounced (sixfold above wild type) compared with medium transcription conditions (260-fold above wild type) and most pronounced (414-fold above wild type) at high transcription levels (Fig. 8 C). We therefore conclude that hyper-recombination in *sem1*Δ and Sem1-TAP strains strongly depends on transcription and resembles the phenotypes seen in other mutants defective in mRNP formation and export (Jimeno et al., 2002; Huertas and Aguilera, 2003).

The accumulation of poly(A)$^+$ RNA, defects in expression of long GC-rich genes, and the observed TAR phenotypes of *sem1Δ* and Sem1-TAP strains suggest that transcription elongation may be impaired. To address this question, we analyzed RNAPII elongation in vivo. RNAPII recruitment was assayed by chromatin immunoprecipitation (ChIP) along the 8 kb–long *YLR454w* gene fused to the *GAL1* promoter (Mason and Struhl, 2005). RNAPII occupancy was determined at the 5′, middle, and a 3′ region of *YLR454w* in wild-type and *sem1Δ* cells. The presence of RNAPII at the middle and 3′ end of the gene was found to be reduced with respect to the 5′ end to ∼50% compared with wild-type levels (Fig. 8 D). This result confirms that transcription elongation is indeed impaired in *sem1Δ* mutants in vivo. Altogether, and consistent with the genetic links, these data demonstrate that like other members

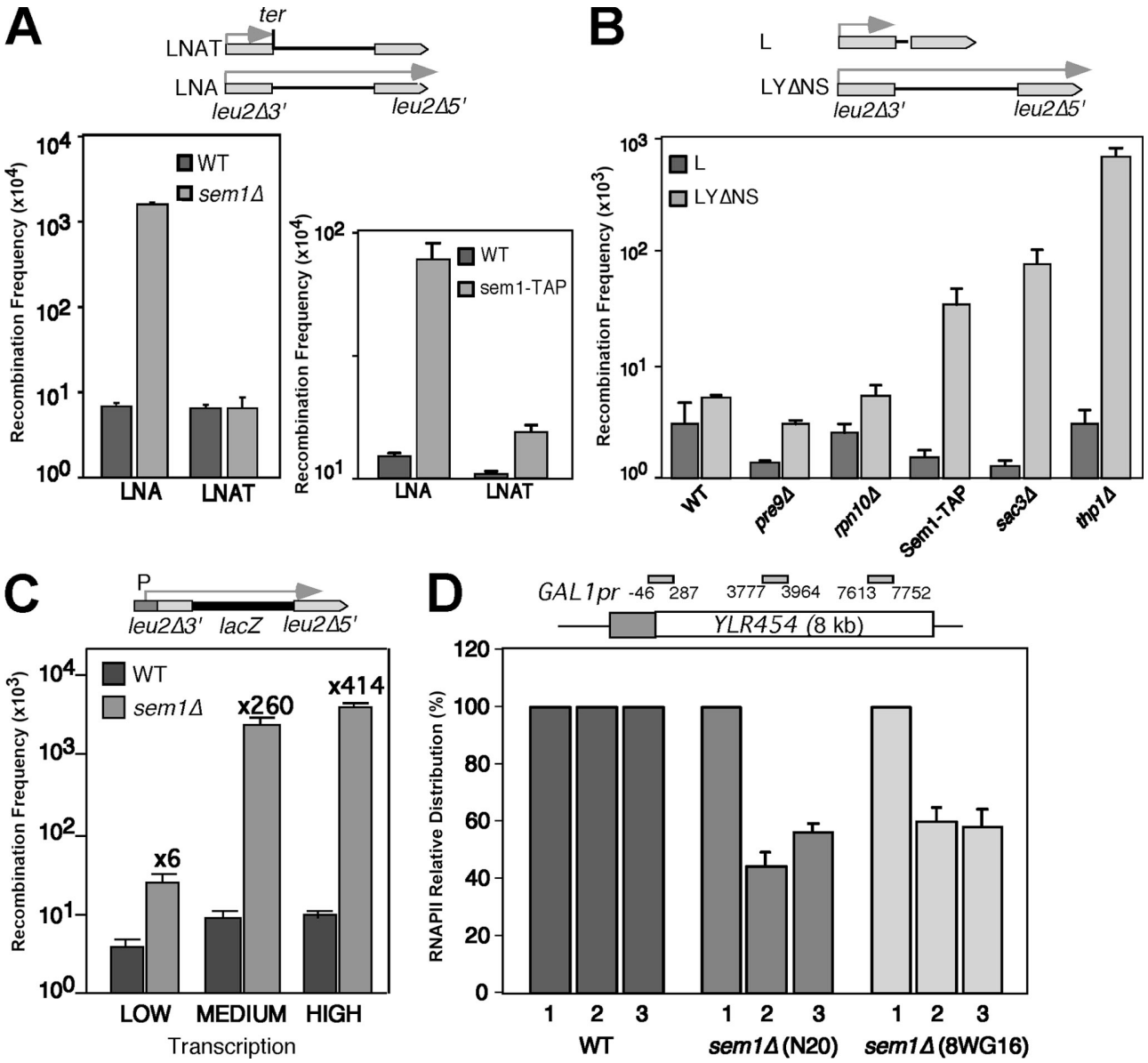

Figure 8. ***sem1Δ* and Sem1-TAP, but not mutants of the RP, induce TAR.** (A and B) Recombination frequency of *sem1Δ*, *sac3Δ*, *thp1Δ*, Sem1-TAP, and RP mutants (*rpn10Δ and pre9Δ*), and an isogenic wild-type strain (BY4741) in the plasmid-borne recombination systems. A small diagram of the systems (not drawn to scale) is shown. Repeats are shown as gray boxes, and gray arrows indicate relevant transcripts produced from the construct. Recombinants were selected as leu$^+$. Median and SD of three independent experiments are shown. (C) Recombination analysis of *sem1Δ* and isogenic wild type in the plasmid-borne systems L-*lacZ* and GL-*lacZ*. Recombination frequencies, plotted as a function of the transcription levels, are shown. "Low" transcription refers to the GL-*lacZ* system, in which the first *leu2* repeat is under the control of the *GAL1* promoter, in strains cultured in 2% glucose; "medium" refers to L-*lacZ*, in which the *leu2* repeat is under its own promoter, in 2% glucose; and "high" refers to GL-*lacZ* in 2% galactose. Other details were as in A. (D) RNAPII occupancy at the *GAL1pr-YLR454w* gene in *sem1Δ* mutant. ChIP analyses (using N20 or 8WG16 anti-RNAPII antibodies) in wild-type (W303-1A) and *sem1Δ* isogenic strains carrying the GAL1pr::*YLR454w* fusion construct located at the endogenous *YLR454w* chromosomal locus are shown. The scheme of the gene and the PCR-amplified fragments are shown. The DNA ratios in the 5′ (1), middle (2), and 3′(3) regions, were calculated from the DNA amount of these regions relative to the intergenic region. The recruitment data shown are first referred to the value of the 5′ region taken as 100% and then relative to the wild-type levels for each region. Median and SD of three independent experiments are shown. WT, isogenic wild-type strain.

of TREX-2, Sem1 likewise functions in transcription elongation and maintenance of genomic integrity.

sem1Δ favors the action of ssDNA-specific human activation-induced cytidine deaminase (AID)

AID is a B cell–specific enzyme essential for Ig somatic hypermutation and class switching. One of its in vivo targets is the S region of Ig genes, in which R loops are formed (Yu et al., 2003). We have recently reported that the heterologous overexpression of human AID strongly increases both mutation and recombination in yeast THO and *thp1Δ* mutants (Gómez-González and Aguilera, 2007; Gonzalez-Aguilera et al., 2008). This increase is consistent with the formation of R loops in THO mutants, where the nontranscribed strand is exposed as ssDNA (Huertas and Aguilera, 2003) and thereby rendered

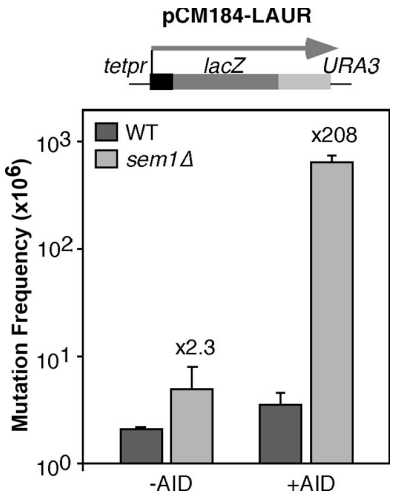

Figure 9. **Spontaneous and AID-induced mutation frequencies in *sem1Δ*.** Analysis of the genetic instability (mutation and recombination) phenotype in W303-1A and *sem1Δ* isogenic strains, using the *tetpr::lacZ-URA3* fusion construct. Ura$^-$ mutants were selected on 5-FOA. The human *AID* gene, present in the p413-GALAID plasmid, was either overexpressed in 2% galactose (+AID) or repressed in 2% glucose (−AID). Median and SD of three independent experiments are shown.

susceptible to mutation by AID. We wondered, therefore, whether *sem1Δ* also stimulates accumulation of mutations caused by AID activity as an indirect way to assess the formation of R loops in this mutant. We used the pLAUR system in which ura$^-$ colonies are selected on 5-fluoroorotic acid (5-FOA). *sem1Δ* only increased the ura$^-$ mutation frequency 2.3-fold above wild-type levels when AID was not expressed (Fig. 9). However, this increase was 208-fold above wild-type levels when AID was overexpressed. Therefore, we can conclude that *sem1Δ* mutants transiently accumulate ssDNA, which can be targeted by AID, in a transcription-dependent manner. This is consistent with the putative presence of R loops in *sem1Δ* mutants, as was described previously (Gómez-González and Aguilera, 2007; González-Aguilera et al., 2008).

Discussion

Previous studies in budding and fission yeasts had identified Sem1 as a bona fide subunit of the RP of the proteasome (Funakoshi et al., 2004; Krogan et al., 2004; Sone et al., 2004). Here, we provide several lines of evidence that in addition to its proteasomal role, Sem1 functions in mRNA export as part of TREX-2. First, we show that Sem1 is the unique nonessential subunit of the RP that is impaired in mRNA export and functionally linked to the mRNA export machinery. Second, like *sac3Δ* and *thp1Δ*, *sem1Δ* mutants are defective in transcription of long GC-rich genes, which leads to transcription-dependent hyper-recombination phenotypes and susceptibility to the mutagenic action of AID (Gallardo and Aguilera, 2001; Tous and Aguilera, 2007; González-Aguilera et al., 2008). Finally, we show that Sem1 specifically coenriches with TREX-2, independently of the RP. The reason why association of Sem1 with TREX-2 was not previously observed appears to be due to the use of Sem1-TAP alleles. The functionality of Sem1-TAP was not previously tested (e.g., in an *sl* relationship). Sem1-TAP is nonfunctional in the mRNA export pathway, as the Sem1-TAP strain showed a defect in mRNA export and, when combined with *mex67* and *mtr2* mutant alleles, was found to be *sl*. Thus, only a combined approach of genetic and biochemical assays was able to unravel the function of Sem1 in mRNA export.

What could be the role of Sem1 in the CSN? The CSN is composed of eight distinct subunits and is highly homologous to the lid subcomplex of the RP. Deletions of members of the CSN complex have been shown to accumulate neddylated cullin Cdc53 (Maytal-Kivity et al., 2002). Functional analysis of the PAM domain containing Csn12 showed that it does not participate in the deneddylation of Cdc53 (Maytal-Kivity et al., 2002). Furthermore, we did not observe any alterations in Cdc53 deneddylation in *sem1Δ* and *ypr045cΔ* strains (Fig. S5). Moreover, both *csn12Δ* and *ypr045cΔ* strains are not defective in mRNA export (Fig. S1 A), which suggests that Sem1 has an additional role in the CSN that is independent of its function in the RP and TREX-2. While this work was under revision, Wilmes et al. (2008) showed that Sem1 coenriches with distinct complexes (RP, TREX-2, and CSN). Furthermore, they showed that the Csn12-Ypr045c-Sem1 subcomplex associates with the splicing machinery and that the *csn12Δ* and *ypr045c* strains were defective in pre-mRNA splicing. Thus, we speculate that the Csn12–Ypr045c–Sem1 subcomplex is likely to affect a yet undetermined activity of the CSN.

What could be the functional role of Sem1 in these three protein complexes? The common feature of the RP, TREX-2, and CSN is the presence of Sac3-GANP and PAM domain–containing subunits (Fig. 9; Hofmann and Bucher, 1998; Ciccarelli et al., 2003; Scheel and Hofmann, 2005). Importantly, Sem1 specifically coenriches with the N+M–Sac3 domain that contains a Sac3-GANP domain and also binds the PAM domain–containing Thp1. Recently, a specific acidic motif in Sem1 has been shown to directly interact with Rpn3 in vitro (Wei et al., 2008). Furthermore, a combination of chemical cross-linking followed by mass spectrometry and yeast two-hybrid analyses of the RP suggests that Sem1 lies in the near vicinity of Rpn3 (PAM) and Rpn12 (Sac3-GANP; Sharon et al., 2006; Gudmundsdottir et al., 2007). These findings have led us to speculate that Sem1 might facilitate interactions between the Sac3-GANP-containing subunit and its PAM domain counterpart. Consistent with this notion, we have observed that the tethering of Thp1 to the NPC is severely affected in *sem1Δ*. Previously, an RP purified from *sem1Δ* cells was shown to be considerably destabilized and defective in ubiquitin-mediated proteasomal degradation (Funakoshi et al., 2004; Sone et al., 2004). Whether Sem1 "glues" the Sac3-GANP and PAM domains together still remains to be determined. Another possibility is that Sem1 stabilizes the PAM domain, which then would facilitate a robust interaction with the Sac3-GANP-containing subunit or vice versa. Previously, Dss1, the human homologue of Sem1, has been implicated in maintaining the correct conformation of BRCA2, as BRCA2 is largely insoluble in absence of Dss1 (Yang et al., 2002; Kojic et al., 2003). Further biochemical work could provide insights into how Sem1 might facilitate complex formation between Sac3-GANP and PAM-containing proteins.

Can Sem1 interact with other protein complexes? Here, the structure of Dss1 in complex with a part of BRCA2 can provide possible insights. Dss1 was shown to bind the helix turn helix motif (helical domain) and an oligonucleotide-binding domain (OB) of BRCA2 in an extended conformation. Dss1 appears to make contacts with numerous residues on the helical domain and the OB surface that is rich in basic, aromatic, and hydrophobic residues (Yang et al., 2002). The Sac3-GANP and PAM domains contain periodic hydrophobic patches followed by conserved positive residues typically found in α-helical structures (Hofmann and Bucher, 1998; Scheel and Hofmann, 2005). Interestingly, Sac3-GANP and PAM domains have neither structural nor sequence homology with the region of BRCA2 that interacts with Sem1. Thus, it is very likely that Sem1 will target multiple folds present in several unrelated protein complexes. Interestingly, alleles of Mex67 and Mtr2 (*mex67-kraa* and *mtr2-33*), which are specifically defective in 60S export (Bassler et al., 2001; Yao et al., 2007), in combination with *sem1Δ* were also found to be *sl* (Fig. 2), which indicates a functional link of Sem1 to export of the large ribosomal subunit. Purification of the complexes associated with human Dss1 has identified the Integrator complex (involved in snRNA processing) in addition to proteasome and the metazoan-specific BRCA2 (Baillat et al., 2005).

A large body of work in mammalian cells has implicated mutations in the tumor suppressor protein BRCA2 in genomic instability. BRCA2 functions in the repair of DSBs by homologous recombination (Gudmundsdottir et al., 2004, 2007; Li et al., 2006). Dss1 has been shown to stabilize BRCA2, and consistently, depletion of either BRCA2 or Dss1 was shown to induce similar phenotypes of genomic instability (Li et al., 2006). Although yeast lacks an obvious homologue of BRCA2, Sem1, as part of the RP, was shown to be important for the repair of DSBs by both homologous recombination and nonhomologous end-joining pathways (Krogan et al., 2004). Our work has uncovered a nonproteosomal role of Sem1 in preventing transcription-associated genomic instability by regulating the integrity of TREX-2. Mutations in genes encoding components of TREX-2, which functions at the interface between transcription and mRNA export, induce transcription-associated hyper-recombination phenotypes that are very similar to *sem1Δ*. We show that, like *thp1*Δ, the *sem1Δ* mutation facilitates the mutagenic action of AID on transcribed DNA. As AID preferentially acts on ssDNA, this supports the idea that in *sem1Δ* mutants, ssDNA regions accumulate during transcription, which is consistent with the possibility of R-loop formation, as observed in THO complex mutants (Gómez-González and Aguilera, 2007). Recently GANP, the human homologue of Sac3, has been shown to suppress hyper-recombination and AID activity in mammalian cells (Yoshida et al., 2007).

Interestingly, several components that directly participate in mRNA export show moonlighting functions. The TREX-2 component Cdc31 performs an additional role in spindle pole body duplication (Fischer et al., 2004). Similarly, the heterodimeric mRNA export factor Mex6-Mtr2 has been shown to be required for proper nuclear export of the large ribosomal subunit (Yao et al., 2007). Recently, the NPC-associated factors Gle1 and Dbp5 have been shown to function in translation (Bolger et al., 2008). Thus, this study adds Sem1 to the list of versatile proteins that function in multiple pathways, in addition to their direct involvement in mRNA export.

Materials and methods

Yeast strains and microbiological methods

Microbiological techniques such as plasmid transformation, mating, sporulation of diploids, and tetrad analysis were done according to standard procedures. Genomic disruptions were performed as described previously (Longtine et al., 1998; Janke et al., 2004). The yeast strains used in this study are given in Table S1.

Affinity purifications

TAP purification of various bait proteins was performed as described previously (Rigaut et al., 1999). The TEV eluates from calmodulin-Sepharose were trichloroacetic acid precipitated, resuspended in SDS sample buffer, and analyzed on an SDS 4–12% gradient polyacrylamide gel (Invitrogen). Antibodies used for Western blotting were monoclonal anti-CBP (1:3,000; Open Biosystems), polyclonal rabbit anti-Sem1 (1:2,000; gifts from the Kobayashi and Jäntti laboratories), and monoclonal anti-Rpt6 (1:5,000; Bio-Concept). For Western blotting, enhanced chemiluminescence detection was performed (GE Healthcare).

Recombination and mutation analysis

Transcription efficiency, recombination, and mutation frequencies were performed as described previously (Gallardo and Aguilera, 2001; Gómez-González and Aguilera, 2007). Mutation frequencies were derived from the mean of three to four median frequencies from two different transformants each and for each genotype tested. Median frequencies were obtained as described previously (Santos-Rosa and Aguilera, 1994) from six independent colonies per transformant.

Miscellaneous

Detection of nuclear accumulation of poly(A)$^+$ RNA by FISH was performed as described previously (Grosshans et al., 2000). Both fixed cells (FISH analyses) and live cells (resuspended in water) were examined by microscopy using a fluorescence microscope (Imager Z1) equipped with a 63× NA 1.4 Plan-Apochromat oil immersion lens, using DICIII, HE-GFP, DAPI, or HECy3 filters (all from Carl Zeiss, Inc.). Images were acquired with an AxioCam MRm camera and AxioVision 4.3 software (Carl Zeiss, Inc.) at 25°C. Northern analyses were performed according to standard procedures with ^{32}P-radiolabeled probes as described previously (Chávez et al., 2000). RNA levels in arbitrary units (A.U.) were obtained in an FLA 3000 (Fujifilm) and were normalized with respect to rRNA levels of each sample.

CHIP analysis

For ChIP experiments, strains were grown in synthetic complete medium (SC), 2% glycerol and 2% lactate to an OD_{660} of 0.5. The culture was split into two; one half was supplemented with 2% glucose (repressed transcription) and the other half with 2% galactose (activated transcription). Samples were taken after 4 h, and ChIP assays were performed as described previously (Mason and Struhl, 2005). Monoclonal anti-Rpb1-CTD antibodies 8WG16 and N20 (Covance), and protein A–Sepharose were used for RNAPII immunoprecipitation. The GFX purification system (GE Healthcare) was used for the last DNA purification step. We used the PCR of the intergenic region at positions 9,716–9,863 of chromosome V as a negative control. Real-time quantitative PCR and calculation of the relative abundance of each DNA fragment were performed as described previously (Huertas et al., 2006). For the evaluation of RNAPII occupancy, data are expressed as the result of two steps of normalization. First, for each strain, we consider the value of the occupancy in the 5′ region as 100%, and the values of the middle and the 3′ region are normalized to the 5′ region value. In the second normalization step, each value of the wild-type strain is taken as 100%. Then, the value of each region is normalized to the value of the corresponding position in the wild-type strain (the percentage that is obtained for the occupancy of RNAPII in each region of the wild type when it is compared with its 5′ region, taken as 100%).

Online supplemental material

Fig. S1 contains additional FISH data showing the absence of poly(A)$^+$ RNA accumulation in deletions of nonessential proteasome components. Fig. S2 reveals that RP components are not genetically linked to mRNA

export. Fig. S3 demonstrates that NPCs remain intact in *sem1Δ* and that targeting of Thp1-GFP is unperturbed in mutants of the RP. Fig. S4 illustrates the various recombination systems used. Fig. S5 contains the Western analysis showing that the Csn12–Sem1–Ypr045c subcomplex is not involved in deneddylation of the cullin Cdc53. Table S1 lists all yeast strains used in this study. Online supplemental material is available at http://www.jcb.org/cgi/content/full/jcb.200810059/DC1.

We are grateful to S. Keränen, J. Jäntti, H. Kobayashi, and H. Berglund for antibodies and reagents. We thank S. Wente, U. Kutay, M. Peter, S. Lutz, D. Kressler, and all members of the Panse laboratory for helpful discussions. We thank C. Ashiono for help with antibody coupling and G. Rabut for help with the Cdc53 blot. We are particularly grateful to G. Wilmes and C. Guthrie for sharing unpublished data.

A. Aguilera is funded by grants from the Spanish Ministry of Science and Education (BFU2006-05260 and BFU2007-28647) and from the Junta de Andalucia (CVI102 and CVI2549). E. Hurt is a recipient of grants from the Deutsche Forschungsgemeinschaft (SFB638 and B3). V.G. Panse is supported by grants from the Swiss National Science Foundation and Swiss Federal Institute of Technology.

Submitted: 9 October 2008
Accepted: 18 February 2009

References

Aguilera, A. 2005. Cotranscriptional mRNP assembly: from the DNA to the nuclear pore. *Curr. Opin. Cell Biol.* 17:242–250.

Aguilera, A., and B. Gómez-González. 2008. Genome instability: a mechanistic view of its causes and consequences. *Nat. Rev. Genet.* 9:204–217.

Baillat, D., M.A. Hakimi, A.M. Naar, A. Shilatifard, N. Cooch, and R. Shiekhattar. 2005. Integrator, a multiprotein mediator of small nuclear RNA processing, associates with the C-terminal repeat of RNA polymerase II. *Cell.* 123:265–276.

Bassler, J., P. Grandi, O. Gadal, T. Lessmann, E. Petfalski, D. Tollervey, J. Lechner, and E. Hurt. 2001. Identification of a 60S preribosomal particle that is closely linked to nuclear export. *Mol. Cell.* 8:517–529.

Bolger, T.A., A.W. Folkmann, E.J. Tran, and S.R. Wente. 2008. The mRNA export factor Gle1 and inositol hexakisphosphate regulate distinct stages of translation. *Cell.* 134:624–633.

Brickner, J.H., and P. Walter. 2004. Gene recruitment of the activated INO1 locus to the nuclear membrane. *PLoS Biol.* 2:e342.

Cabal, G.G., A. Genovesio, S. Rodriguez-Navarro, C. Zimmer, O. Gadal, A. Lesne, H. Buc, F. Feuerbach-Fournier, J.C. Olivo-Marin, E.C. Hurt, and U. Nehrbass. 2006. SAGA interacting factors confine sub-diffusion of transcribed genes to the nuclear envelope. *Nature.* 441:770–773.

Casolari, J.M., C.R. Brown, S. Komili, J. West, H. Hieronymus, and P.A. Silver. 2004. Genome-wide localization of the nuclear transport machinery couples transcriptional status and nuclear organization. *Cell.* 117:427–439.

Chávez, S., T. Beilharz, A.G. Rondón, H. Erdjument-Bromage, P. Tempst, J.Q. Svejstrup, T. Lithgow, and A. Aguilera. 2000. A protein complex containing Tho2, Hpr1, Mft1 and a novel protein, Thp2, connects transcription elongation with mitotic recombination in *Saccharomyces cerevisiae*. *EMBO J.* 19:5824–5834.

Ciccarelli, F.D., E. Izaurralde, and P. Bork. 2003. The PAM domain, a multiprotein complex-associated module with an all-alpha-helix fold. *BMC Bioinformatics.* 4:64.

Cole, C.N., and J.J. Scarcelli. 2006. Transport of messenger RNA from the nucleus to the cytoplasm. *Curr. Opin. Cell Biol.* 18:299–306.

Duncan, K., J.G. Umen, and C. Guthrie. 2000. A putative ubiquitin ligase required for efficient mRNA export differentially affects hnRNP transport. *Curr. Biol.* 10:687–696.

Fischer, T., K. Strässer, A. Rácz, S. Rodriguez-Navarro, M. Oppizzi, P. Ihrig, J. Lechner, and E. Hurt. 2002. The mRNA export machinery requires the novel Sac3p-Thp1p complex to dock at the nucleoplasmic entrance of the nuclear pores. *EMBO J.* 21:5843–5852.

Fischer, T., S. Rodríguez-Navarro, G. Pereira, A. Rácz, E. Schiebel, and E. Hurt. 2004. Yeast centrin Cdc31 is linked to the nuclear mRNA export machinery. *Nat. Cell Biol.* 6:840–848.

Funakoshi, M., X. Li, I. Velichutina, M. Hochstrasser, and H. Kobayashi. 2004. Sem1, the yeast ortholog of a human BRCA2-binding protein, is a component of the proteasome regulatory particle that enhances proteasome stability. *J. Cell Sci.* 117:6447–6454.

Gallardo, M. 2003. Nab2p and the Thp1p-Sac3p complex functionally interact at the interface between transcription and mRNA metabolism. *J. Biol. Chem.* 278:24225–24232.

Gallardo, M., and A. Aguilera. 2001. A new hyperrecombination mutation identifies a novel yeast gene, THP1, connecting transcription elongation with mitotic recombination. *Genetics.* 157:79–89.

Gómez-González, B., and A. Aguilera. 2007. Activation-induced cytidine deaminase action is strongly stimulated by mutations of the THO complex. *Proc. Natl. Acad. Sci. USA.* 104:8409–8414.

Gonzalez-Aguilera, C., C. Tous, B. Gomez-Gonzalez, P. Huertas, R. Luna, and A. Aguilera. 2008. The THP1-SAC3-SUS1-CDC31 complex works in transcription elongation-mRNA export preventing RNA-mediated genome instability. *Mol. Biol. Cell.* 19:4310–4318.

Grosshans, H., E. Hurt, and G. Simos. 2000. An aminoacylation-dependent nuclear tRNA export pathway in yeast. *Genes Dev.* 14:830–840.

Gudmundsdottir, K., C.J. Lord, E. Witt, A.N. Tutt, and A. Ashworth. 2004. DSS1 is required for RAD51 focus formation and genomic stability in mammalian cells. *EMBO Rep.* 5:989–993.

Gudmundsdottir, K., C. Lord, and A. Ashworth. 2007. The proteasome is involved in determining differential utilization of double-strand break repair pathways. *Oncogene.* 26:7601–7606.

Hofmann, K., and P. Bucher. 1998. The PCI domain: a common theme in three multiprotein complexes. *Trends Biochem. Sci.* 23:204–205.

Huertas, P., and A. Aguilera. 2003. Cotranscriptionally formed DNA: RNA hybrids mediate transcription elongation impairment and transcription-associated recombination. *Mol. Cell.* 12:711–721.

Huertas, P., M.L. García-Rubio, R.E. Wellinger, R. Luna, and A. Aguilera. 2006. An hpr1 point mutation that impairs transcription and mRNP biogenesis without increasing recombination. *Mol. Cell. Biol.* 26:7451–7465.

Janke, C., M.M. Magiera, N. Rathfelder, C. Taxis, S. Reber, H. Maekawa, A. Moreno-Borchart, G. Doenges, E. Schwob, E. Schiebel, and M. Knop. 2004. A versatile toolbox for PCR-based tagging of yeast genes: new fluorescent proteins, more markers and promoter substitution cassettes. *Yeast.* 21:947–962.

Jäntti, J., J. Lahdenranta, V.M. Olkkonen, H. Söderlund, and S. Keränen. 1999. SEM1, a homologue of the split hand/split foot malformation candidate gene Dss1, regulates exocytosis and pseudohyphal differentiation in yeast. *Proc. Natl. Acad. Sci. USA.* 96:909–914.

Jimeno, S., A.G. Rondón, R. Luna, and A. Aguilera. 2002. The yeast THO complex and mRNA export factors link RNA metabolism with transcription and genome instability. *EMBO J.* 21:3526–3535.

Jossé, L., M.E. Harley, I.M. Pires, and D.A. Hughes. 2006. Fission yeast Dss1 associates with the proteasome and is required for efficient ubiquitin-dependent proteolysis. *Biochem. J.* 393:303–309.

Köhler, A., and E. Hurt. 2007. Exporting RNA from the nucleus to the cytoplasm. *Nat. Rev. Mol. Cell Biol.* 8:761–773.

Kojic, M., H. Yang, C.F. Kostrub, N.P. Pavletich, and W.K. Holloman. 2003. The BRCA2-interacting protein DSS1 is vital for DNA repair, recombination, and genome stability in *Ustilago maydis*. *Mol. Cell.* 12:1043–1049.

Kojic, M., Q. Zhou, M. Lisby, and W.K. Holloman. 2005. Brh2-Dss1 interplay enables properly controlled recombination in *Ustilago maydis*. *Mol. Cell. Biol.* 25:2547–2557.

Krogan, N.J., M. Lam, J. Fillingham, M. Keogh, M. Gebbia, J. Li, N. Datta, G. Cagney, S. Buratowski, and A. Emili. 2004. Proteasome involvement in the repair of DNA double-strand breaks. *Mol. Cell.* 16:1027–1034.

Krogan, N.J., G. Cagney, H. Yu, G. Zhong, X. Guo, A. Ignatchenko, J. Li, S. Pu, N. Datta, A.P. Tikuisis, et al. 2006. Global landscape of protein complexes in the yeast *Saccharomyces cerevisiae*. *Nature.* 440:637–643.

Kurshakova, M.M., A.N. Krasnov, D.V. Kopytova, Y.V. Shidlovskii, J.V. Nikolenko, E.N. Nabirochkina, D. Spehner, P. Schultz, L. Tora, and S.G. Georgieva. 2007. SAGA and a novel *Drosophila* export complex anchor efficient transcription and mRNA export to NPC. *EMBO J.* 26:4956–4965.

Lee, D.H., and A.L. Goldberg. 1998. Proteasome inhibitors: valuable new tools for cell biologists. *Trends Cell Biol.* 8:397–403.

Li, J., C. Zou, Y. Bai, D. Wazer, V. Band, and Q. Gao. 2006. DSS1 is required for the stability of BRCA2. *Oncogene.* 25:1186–1194.

Longtine, M.S., A. McKenzie, D.J. Demarini, N.G. Shah, A. Wach, A. Brachat, P. Philippsen, and J.R. Pringle. 1998. Additional modules for versatile and economical PCR-based gene deletion and modification in *Saccharomyces cerevisiae*. *Yeast.* 14:953–961.

Mannen, T., T. Andoh, and T. Tani. 2008. Dss1 associating with the proteasome functions in selective nuclear mRNA export in yeast. *Biochem. Biophys. Res. Commun.* 365:664–671.

Marston, N.J., W.J. Richards, D. Hughes, D. Bertwistle, C.J. Marshall, and A. Ashworth. 1999. Interaction between the product of the breast cancer susceptibility gene BRCA2 and DSS1, a protein functionally conserved from yeast to mammals. *Mol. Cell. Biol.* 19:4633–4642.

Mason, P.B., and K. Struhl. 2005. Distinction and relationship between elongation rate and processivity of RNA polymerase II in vivo. *Mol. Cell.* 17:831–840.

Maytal-Kivity, V., R. Piran, E. Pick, K. Hofmann, and M.H. Glickman. 2002. COP9 signalosome components play a role in the mating pheromone response of *S. cerevisiae*. *EMBO Rep.* 3:1215–1221.

Neumann, S., E. Petfalski, B. Brugger, H. Grosshans, F. Wieland, D. Tollervey, and E. Hurt. 2003. Formation and nuclear export of tRNA, rRNA and mRNA is regulated by the ubiquitin ligase Rsp5p. *EMBO Rep.* 4:1156–1162.

Reed, R., and H. Cheng. 2005. TREX, SR proteins and export of mRNA. *Curr. Opin. Cell Biol.* 17:269–273.

Rigaut, G., A. Shevchenko, B. Rutz, M. Wilm, M. Mann, and B. Séraphin. 1999. A generic protein purification method for protein complex characterization and proteome exploration. *Nat. Biotechnol.* 17:1030–1032.

Rodríguez-Navarro, S., T. Fischer, M.J. Luo, O. Antúnez, S. Brettschneider, J. Lechner, J.E. Pérez-Ortín, R. Reed, and E. Hurt. 2004. Sus1, a functional component of the SAGA histone acetylase complex and the nuclear pore-associated mRNA export machinery. *Cell.* 116:75–86.

Santos-Rosa, H., and A. Aguilera. 1994. Increase in incidence of chromosome instability and non-conservative recombination between repeats in *Saccharomyces cerevisiae* hpr1 delta strains. *Mol. Gen. Genet.* 245:224–236.

Scheel, H., and K. Hofmann. 2005. Prediction of a common structural scaffold for proteasome lid, COP9-signalosome and eIF3 complexes. *BMC Bioinformatics.* 6:71.

Sharon, M., T. Taverner, X. Ambroggio, R. Deshaies, and C. Robinson. 2006. Structural organization of the 19S proteasome lid: insights from MS of intact complexes. *PLoS Biol.* 4:e267.

Sommer, P., and U. Nehrbass. 2005. Quality control of messenger ribonucleoprotein particles in the nucleus and at the pore. *Curr. Opin. Cell Biol.* 17:294–301.

Sone, T., Y. Saeki, A. Toh-e, and H. Yokosawa. 2004. Sem1p is a novel subunit of the 26 S proteasome from *Saccharomyces cerevisiae*. *J. Biol. Chem.* 279:28807–28816.

Suntharalingam, M., and S.R. Wente. 2003. Peering through the pore: nuclear pore complex structure, assembly, and function. *Dev. Cell.* 4:775–789.

Taddei, A., G. Van Houwe, F. Hediger, V. Kalck, F. Cubizolles, H. Schober, and S. Gasser. 2006. Nuclear pore association confers optimal expression levels for an inducible yeast gene. *Nature.* 441:774–778.

Thakurta, A.G., G. Gopal, J. Yoon, L. Kozak, and R. Dhar. 2005. Homolog of BRCA2-interacting Dss1p and Uap56p link Mlo3p and Rae1p for mRNA export in fission yeast. *EMBO J.* 24:2512–2523.

Tous, C., and A. Aguilera. 2007. Impairment of transcription elongation by R-loops in vitro. *Biochem. Biophys. Res. Commun.* 360:428–432.

Voynov, V., K.J. Verstrepen, A. Jansen, V.M. Runner, S. Buratowski, and G.R. Fink. 2006. Genes with internal repeats require the THO complex for transcription. *Proc. Natl. Acad. Sci. USA.* 103:14423–14428.

Wei, S.J., J.G. Williams, H. Dang, T.A. Darden, B.L. Betz, M.M. Humble, F.M. Chang, C.S. Trempus, K. Johnson, R.E. Cannon, and R.W. Tennant. 2008. Identification of a specific motif of the DSS1 protein required for proteasome interaction and p53 protein degradation. *J. Mol. Biol.* 383:693–712.

Wilmes, G.M., M. Bergkessel, S. Bandyopadhyay, M. Shales, H. Braberg, G. Cagney, S.R. Collins, G.B. Whitworth, T.L. Kress, J.S. Weissman, et al. 2008. A genetic interaction map of RNA-processing factors reveals links between Sem1/Dss1-containing complexes and mRNA export and splicing. *Mol. Cell.* 32:735–746.

Yang, H., P.D. Jeffrey, J. Miller, E. Kinnucan, and Y. Sun. 2002. BRCA2 function in DNA binding and recombination from a BRCA2-DSS1-ssDNA structure. *Science.* 297:1837–1848.

Yao, W., D. Roser, A. Köhler, B. Bradatsch, J. Bassler, and E. Hurt. 2007. Nuclear export of ribosomal 60S subunits by the general mRNA export receptor Mex67-Mtr2. *Mol. Cell.* 26:51–62.

Yoshida, M., K. Kuwahara, T. Shimasaki, N. Nakagata, M. Matsuoka, and N. Sakaguchi. 2007. GANP suppresses DNA recombination, measured by direct-repeat beta-galactosidase gene construct, but does not suppress the type of recombination applying to immunoglobulin genes in mammalian cells. *Genes Cells.* 12:1205–1213.

Yu, K., F. Chedin, C.L. Hsieh, T.E. Wilson, and M.R. Lieber. 2003. R-loops at immunoglobulin class switch regions in the chromosomes of stimulated B cells. *Nat. Immunol.* 4:442–451.